Thermal decomposition of nitrogen trifluoride in shock waves

Cite as: J. Chem. Phys. **65**, 4202 (1976); https://doi.org/10.1063/1.432827
Published Online: 28 August 2008

P. J. Evans, and E. Tschuikow-Roux

Thermal decomposition of nitrogen trifluoride in shock waves

P. J. Evans* and E. Tschuikow-Roux

Department of Chemistry, University of Calgary, Calgary, Alberta T2N 1N4, Canada
(Received 19 April 1976)

The thermal decomposition of nitrogen trifluoride has been reinvestigated behind incident shock waves in dilute (1%) NF_3/Ar mixtures over the temperature range 1150–1530 K and at 0.80–1.81 atm total pressures. The reaction kinetics were followed by monitoring NF_2 radical concentrations in absorption at 260 nm. In several experiments, the infrared emission at 5.17 μ was also monitored. Under the experimental conditions used, the reversible dissociation $NF_3+M \rightleftharpoons NF_2+F+M$ is known to be first order in both NF_3 and Ar concentrations, and the low pressure limit second-order rate constant was found to be $k_1(\text{cm}^3\ \text{mol}^{-1}\ \text{s}^{-1}) = 10^{16.61\pm0.13} \times \exp[-(48.0\pm0.8\ \text{kcal mol}^{-1})/RT]$ using an approximate iterative procedure. A numerical solution of the differential rate equation yielded comparable results. The temperature dependence of the absorption coefficient for NF_2 and the equilibrium constant were also determined.

I. INTRODUCTION

The thermal decomposition of nitrogen trifluoride has been reported in several previous studies.[1–3] MacFadden and Tschuikow-Roux[1] (MT-R) showed that for dilute (1%) NF_3/Ar mixtures in the temperature range 1050–1400 K and 2.7–6.0 atm total pressure the principal reaction is the reversible dissociation $NF_3 + M \rightleftharpoons NF_2 + F + M$. The reaction kinetics were followed by monitoring the NF_2 radical concentration in absorption behind incident shock waves, and it was shown that the rate was first order in NF_3 and Ar concentrations. It was noted that the *observed* activation energy of 30.1 kcal mol^{-1} was much lower than the bond dissociation energy $D(F_2N-F) = 57$ kcal mol^{-1},[4] an observation which could not be adequately correlated with theoretical models. MT-R nevertheless concluded that their rate expression provided an empirical relation for the rate of dissociation of NF_3.

The work by Schott *et al.*[2] dealt mainly with the exploratory reaction kinetics of shock heated NF_3/H_2 and N_2F_4/H_2 mixtures in argon, and no Arrhenius parameters were reported for the thermal decomposition of pure NF_3 in argon. However, a value of the second-order rate constant for NF_3 decomposition at 1400 K and 0.7 atm total pressure was given by Schott *et al.* as $k = 4.75\times10^8$ cm^3 mol^{-1} s^{-1}, which compared within a factor of 2 with the value calculated from the Arrhenius expression of MT-R.

More recently, Dorko *et al.*[3] studied the decomposition of nitrogen trifluoride over a wide range of pressures (0.8–60 atm) and much higher temperature (1500–2400 K) in the reflected shock region by monitoring the emission decay from the $\nu_1+\nu_3$ combination band of NF_3 at 5.18 μ. The reaction kinetics were analyzed in terms of the Lindemann mechanism of unimolecular reactions and the first-order rate constants when divided by total concentrations yielded the Arrhenius expression $k = 10^{14.7} \exp[-(56.3\ \text{kcal mol}^{-1})/RT]$ cm^3 mol^{-1} s^{-1}. The proximity of the activation energy to the N–F dissociation energy in NF_3 was cited by Dorko *et al.* in support of their data. This result will be discussed further below, but it may be noted here that the Arrhenius expression over the entire pressure dependent domain is of doubtful utility. Furthermore, the numerical values of the rate constants in the work of Dorko *et al.* are more than two orders of magnitude lower than those reported by other investigators. In view of these discrepancies it was felt appropriate to reinvestigate the shock tube decomposition of nitrogen trifluoride. The spectrophotometric method employed was similar to that used in the earlier study.[1]

II. EXPERIMENTAL SECTION

A detailed description of the aluminum shock tube (80 mm i.d.) has been reported previously.[5] In the present work, the lengths of the driver and driven sections were 1.83 and 4.47 m, respectively. Aluminum diaphragms of 0.215 mm thickness were used in most experiments.

Incident shock velocities were measured by means of three Kistler pressure transducers (Model 603 A) which were located 0.40, 0.60, and 0.80 m from the endplate. The signals from the transducers were fed to two universal counters (Hewlett–Packard, Model 5325 A), which provided a direct measurement of the shock transit times.

The reaction kinetics were monitored by following the light absorption at 260 nm as a function of time. The absorption at this wavelength has been shown to be due to the NF_2 radical.[6(a)] All absorption measurements were made 38 mm downstream from the last pressure transducer.

The spectrophotometric detection system consisted of a xenon arc lamp (Hanovia, Model 538 C-1), two quartz lenses to focus the light beam, two 1 mm slits at each window of the shock tube, a 0.35 m plane grating monochromator (Heath, Model EU-700), and a photomultiplier module (Heath, Model EU-701-30). The latter unit was equipped with an RCA 1P28A photomultiplier tube. The photomultiplier output was passed through a preamplifier (Analog Devices, Model 46J) and displayed on an oscilloscope where it was recorded photographically. The effective time resolution of the above detection system was determined to be the transit time of the shock front across the 1 mm slits, which

was typically less than 1 μs.

In most experiments, the photomultiplier output was recorded on two oscilloscopes which had different time base settings. The oscilloscope with the faster sweep rate was used for the rate constant determination, while the one with the slower setting was used to determine the NF_2 absorption when the reaction had reached equilibrium.

In several experiments, the progress of the reaction was also monitored by means of infrared emission simultaneously with the ultraviolet absorption measurements. For these experiments, a liquid nitrogen cooled InSb detector (Texas Instruments) was used to monitor the emission. An interference filter centered at 5.17 μ with a 0.22 μ bandwidth was used to select the wavelength region of interest.

Nitrogen trifluoride (Air Products) of 99.8% purity was used without further purification. A mass spectrum of this gas indicated trace impurities of N_2 and N_2O. Argon (Canadian Liquid Air) of 99.995% purity was used as a diluent gas. Reaction mixtures of 1% NF_3 in argon were prepared in stainless steel tanks and allowed to mix prior to use. Mass spectrometric analysis of the reaction mixtures indicated the absence of major or unexpected impurities. Tetrafluorohydrazine (Air Products) of 99.8% purity was used to prepare the 0.25% N_2F_4 in argon mixtures.

Frozen and equilibrium conditions behind the incident shock wave were calculated from the shock velocity and initial test gas composition using a NASA computer program[7] and JANAF thermochemical data.[8]

III. KINETIC ANALYSIS

The method of data reduction used in this study is similar to that detailed previously,[1,5] and only a brief description is given here. The primary reaction under the conditions of the present study has been shown[1,2] to be the reversible reaction

$$NF_3 + M \underset{k_{-1}}{\overset{k_1}{\rightleftharpoons}} NF_2 + F + M. \qquad \text{(R1)}$$

Schott *et al.*[2] have shown that the inclusion of the reactions

$$2F \rightleftharpoons F_2, \qquad \text{(R2)}$$

$$NF_2 \rightleftharpoons NF + F, \qquad \text{(R3)}$$

$$NF \rightleftharpoons N + F, \qquad \text{(R4)}$$

in postshock equilibrium calculations resulted in NF_2 concentrations that were only slightly different from those calculated without these reactions. Similar equilibrium calculations performed in the course of this work confirmed this result.

The rate expression for the decomposition of NF_3 via Reaction (R1), is given by

$$-\frac{d[NF_3]}{dt_p} = k_1[NF_3][M] - k_{-1}[NF_2][F][M], \qquad (1)$$

where the concentrations refer to the region behind the incident shock, [M] is the total gas concentration, and t_p is the particle time. Using the relations $\alpha = [NF_2]/\rho_{21}[NF_3]_1$, $K_c = k_1/k_{-1}$, and $t_p = \rho_{21}t$, where α is the fraction of NF_3 dissociated, ρ_{21} is the density ratio across the shock front, K_c is the equilibrium constant, t is the laboratory time, and the concentration subscript 1 refers to the region ahead of the shock front, Eq. (1) can be written as

$$\frac{d\alpha}{dt} = k_1\rho_{21}^2[M]_1(1-\alpha) - k_1\rho_{21}^3[M]_1[NF_3]_1\alpha^2/K_c. \qquad (2)$$

The integration of Eq. (2) yields[1]

$$\ln\left[\frac{1+\alpha\psi^{-1}}{1-\alpha\phi^{-1}}\right] = a\rho_{21}^2[M]_1 k_1 t, \quad (\alpha < \phi); \qquad (3)$$

where $a = (1+4/b)^{1/2}$, $b = K_c/\rho_{21}[NF_3]_1$, $\psi = (a+1)b/2$, and $\phi = (a-1)b/2$. From the linear plots of $\ln[(1+\alpha\psi^{-1})/(1-\alpha\varphi^{-1})]$ vs t, the rate constant for the forward reaction, k_1, can be calculated.

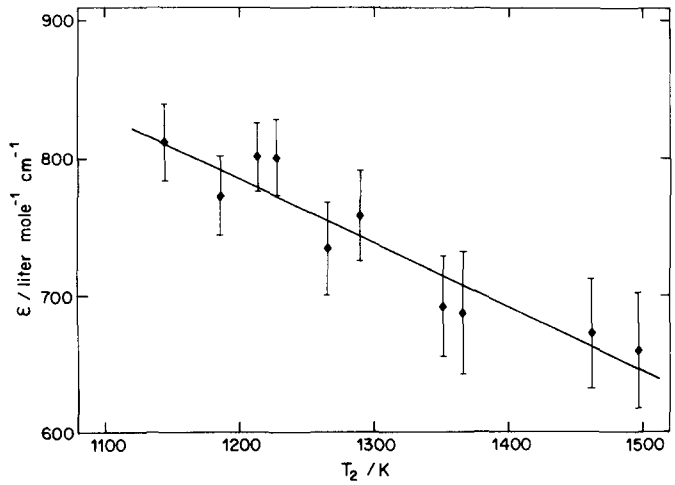

FIG. 1. Plot of absorption coefficient ϵ vs incident shock temperature T_2.

IV. RESULTS AND DISCUSSION

A. Absorption coefficient of NF_2

The absorption coefficient of NF_2 in the temperature range 1140–1500 K was measured in a series of shock tube experiments on a 0.25% N_2F_4–99.75% Ar mixture. In the above temperature range the N_2F_4 is completely dissociated to NF_2, and the absorption coefficient of NF_2 was calculated by means of the relation

$$\ln(I_0/I) = \epsilon[NF_2]l, \qquad (4)$$

where I_0 and I are the incident and transmitted light intensities respectively, ϵ is the absorption coefficient, and l is the path length of the absorbing medium. The results of these experiments are presented in Fig. 1 as a plot of ϵ vs temperature behind the incident shock, T_2. The line shown in this figure is a least squares fit to the experimental points and over the temperature range can be represented by the equation

$$\epsilon(1\,\text{mol}^{-1}\,\text{cm}^{-1}) = 1344.5 - 0.4659T_2. \qquad (5)$$

In addition to the above shock tube experiments, two room temperature measurements of the absorption

TABLE I. Absorption coefficients for NF_2.

ϵ(liter mol^{-1} cm^{-1})	Method of measurement	Temperature range (K)	Ref.
1089	Spectrophotometric N_2F_4/NF_2 equilibrium	298	6
537	Shock heated N_2F_4–Ar mixtures	358–701	9
276–317	Shock heated N_2F_4–Ar mixtures	554–738	10
309	N_2F_4 in heated flow system	293	11
603	Shock heated N_2F_4–Ar mixtures	800–1400	1
$\leq$550	Shock heated N_2F_4–Ar mixtures	527–1935	2
1070	Spectrophotometric N_2F_4/NF_2 equilibrium	298	This work
1344.5–0.4659T	Shock heated N_2F_4–Ar mixtures	1140–1500	This work

spectrum of NF_2 in the $N_2F_4 \rightleftharpoons 2NF_2$ system[6] were performed on a Cary 15 spectrometer equipped with a 10 cm quartz gas cell. The total pressures of N_2F_4 in these experiments were 121 and 400 Torr. By using Eq. (4) and calculating equilibrium NF_2 concentrations from JANAF equilibrium constants, ϵ values of 1057 and 1082 l mol^{-1} cm^{-1} were obtained. These values compare favorably with the value of 1206 l mol^{-1} cm^{-1} calculated from Eq. (5) at 298 K (linear extrapolation). Thus the two independent determinations are in satisfactory agreement.

The above room temperature results are also in good agreement with the first measured value of the NF_2 absorption coefficient by Johnson and Colburn.[6] These authors reduced their data by means of the decadic form of the Beer–Lambert law[6(b)]

$$\log_{10}(I_0/I) = \kappa[NF_2]\,l, \tag{6}$$

where $\kappa = \epsilon/2.303$ is the absorptivity. They obtained a value of $\kappa = 565$ l mol^{-1} cm^{-1} at 298 K based on an experimentally determined equilibrium constant for the reaction $N_2F_4 \rightleftharpoons 2NF_2$. If the above absorptivity is recalculated using the JANAF data, a value of 473 l mol^{-1} cm^{-1} is obtained. The absorptivity of 473 l mol^{-1} cm^{-1} is equivalent to an absorption coefficient $\epsilon = 1089$ l mol^{-1} cm^{-1}. Thus the room temperature results of the present study are in close agreement with the earlier results of Johnson and Colburn.[6]

Other published values of the NF_2 absorption coefficient are listed in Table I. The values given in Refs. 10 and 11 were determined by using broadband interference filters as a means of wavelength selection. Since the use of such filters violates the conditions required for the application of Beer's law,[12] the values from these sources cannot be compared directly with the other values listed in Table I. Therefore, these two results will not be considered further. The results of Refs. 1, 2, and 9, which are all of a similar magnitude, do not agree with those obtained in the present study or with the room temperature value of Johnson and Colburn[6]; the apparent agreement cited[1,2,9] with the value of the latter authors ($\kappa = 565$ l mol^{-1} cm^{-1}) is fortuitous in view of the difference in logarithmic base used.

The difference between the ϵ values reported by previous investigators,[1,2,9] and those of the present work, is attributed to the higher NF_2 concentrations used in the earlier studies, in as much as the variation of optical density with concentration becomes nonlinear, and hence the Beer–Lambert law is no longer applicable. The occurrence of this effect in the case of NF_2 has been reported by Schott *et al.* (cf. Fig. 3, Ref. 9).

B. Thermochemical data

The equilibrium NF_2 concentrations determined from the experimental data by using Eqs. (4) and (5) were significantly different from the values computed using the JANAF thermochemical data.[8] This fact suggests that errors may exist in the JANAF data for one or more of the species involved in Reaction (R1).

If the equilibrium transmitted light intensities from the NF_3 experiments are reduced with the use of Eqs. (4) and (5) to give NF_2 concentrations, equilibrium constants K_c for Reaction (R1) can be calculated from the relations

$$K_c = [NF_2]_{eq}\,[F]_{eq}/[NF_3]_{eq}, \tag{7}$$

$$[NF_2]_{eq} = [F]_{eq} = (\epsilon l)^{-1} \ln(I_0/I), \tag{8}$$

$$[NF_3]_{eq} = \rho_{21,eq}[NF_3]_1 - [NF_2]_{eq}, \tag{9}$$

where the subscript eq denotes conditions at equilibrium and $\rho_{21,eq}$ is the corresponding density ratio across the shock front. The results of these calculations are presented in Fig. 2, where $\log_{10}K_c$ is plotted against the inverse of the equilibrium temperature $T_{2,eq}$. The least squares line through the data points is represented by the equation

$$\log_{10}K_c = 6.1096 - 12951/T_{2,eq}. \tag{10}$$

Also plotted in Fig. 2 is the equilibrium constant for Reaction (R1) determined from the JANAF tables.[8] Within the scatter of the experimental data, the two lines are parallel and the displacement corresponds to a Gibbs free energy difference of ~2.6 kcal mol^{-1}.

An examination of the JANAF tabulations[8] for the species involved in Reaction (R1) revealed that the NF_3 and F atom data contains relatively small errors. However, this was not the case with NF_2, and the previously discussed differences are attributed to uncertainties associated with the thermochemical data of this species.

In the following rate constant analysis, Eq. (10) was used to determine values of the equilibrium constant.

C. Rate constant

The procedure outlined in Sec. III for obtaining the second-order rate constant from the integrated rate expression given by Eq. (3) is only exact for constant temperature and density conditions in the reaction zone (i.e., frozen conditions). Since the latter criteria were

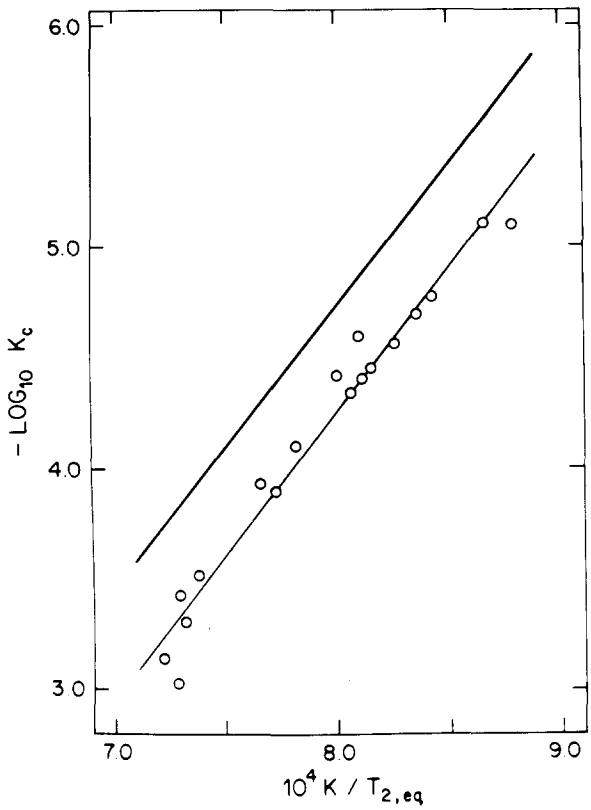

FIG. 2. Temperature dependence of the measured equilibrium constant $K_c(\text{mol l}^{-1})$ for the reaction $NF_3 \rightleftharpoons NF_2 + F$. Upper line based on JANAF thermochemical data.

not strictly satisfied in the present experiments, two methods were employed to reduce the data, both of which take into account the endothermicity of the reaction.

Both methods require expressions which describe the variation of gas properties as the reaction progresses. With the aid of the aforementioned computer program,[7] it was possible to calculate density ratio and temperature changes as a function of the degree of dissociation α. For the 1% NF_3 in argon mixture, the least squares expressions for these changes were found to be

$$-\Delta T_2 = 0.5560 + 95.57\alpha - 1.905\alpha^2 \tag{11}$$

and

$$\Delta\rho_{21} = 0.003389 + 0.3900\alpha - 0.09225\alpha^2, \tag{12}$$

where $-\Delta T_2$ is the temperature decrease and $\Delta\rho_{21}$ is the density increase corresponding to the degree of dissociation α. The temperature and density ratio in the reaction zone are now determined by means of the relations

$$T_2 = T_{2,fz} + \Delta T_2, \tag{13}$$

$$\rho_{21} = \rho_{21,fz} + \Delta\rho_{21}, \tag{14}$$

where $T_{2,fz}$ and $\rho_{21,fz}$ are the frozen values of the temperature and density ratio, respectively, and T_2 and ρ_{21} are the instantaneous values. Since the NF_2 absorption profiles yield values of α as a function of time, Eqs. (11)–(14) also express the time dependence of the temperature and density ratio.

Initially, the experimental absorption profiles were reduced by an approximate iterative procedure based on Eq. (3). By using Eqs. (4), (5), and (10)–(14), values of a, b, ψ^{-1}, ϕ^{-1}, and ρ_{21} in Eq. (3) were evaluated at each measured point of the experimental profiles. By this means, the left and right hand sides of Eq. (3) were evaluated at each point and plots of $\ln[(1+\alpha\psi^{-1})/(1-\alpha\phi^{-1})]$ vs $a\rho_{21}^2[M]_1 t$ were constructed.

A typical oscilloscope record of the NF_2 radical absorption and the base line corresponding to zero transmission is shown in Fig. 3 and a plot of Eq. (3) for this experiment is presented in Fig. 4. The slope of the

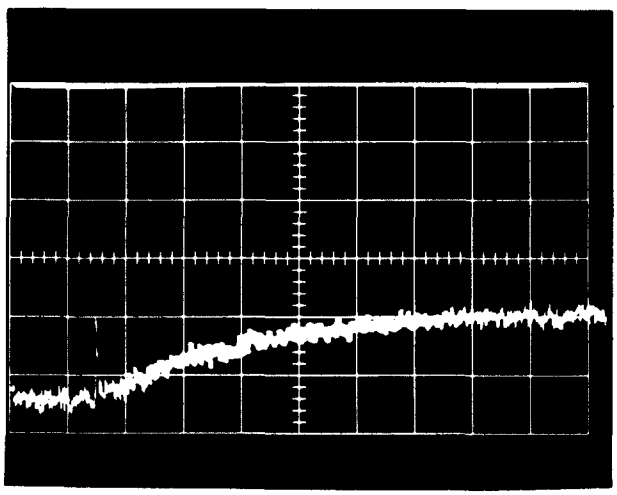

FIG. 3. Sample oscillogram of NF_2 absorption at 260 nm for 1% NF_3–Ar mixture. The base line corresponding to zero transmission (top of graticule) is also shown. For this experiment, $p_1 = 60$ torr, $T_1 = 297$ K, $u_1 = 1070\ \text{m s}^{-1}$ and $T_{2;fz} = 1282$ K. Vertical Scale = 1.0 V div^{-1}, horizontal scale = 20 μs div^{-1}.

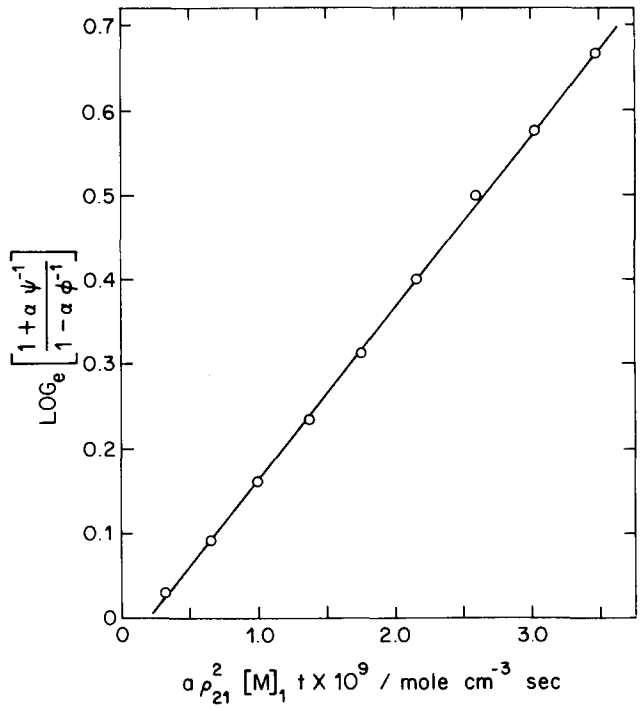

FIG. 4. Plot of $\ln[(1+\alpha\psi^{-1})/(1-\alpha\phi^{-1})]$ vs $a\rho_{21}^2[M]_1 t$ for the experimental profile presented in Fig. 3.

TABLE II. Rate constant results.

W_1^a	$[M]_1 \times 10^6$ (mol cm^{-3})	$T_{2,fz}$ (K)	T_m (K)	$k_1 \times 10^{-7}$ (cm^3 mol^{-1} s^{-1})
3.17	4.23	1149	1144	3.11
3.18	4.25	1156	1151	3.22
3.21	4.07	1168	1162	3.91
3.24	3.97	1191	1184	3.78
3.28	3.87	1204	1196	7.45
3.30	3.71	1217	1209	9.28
3.33	3.55	1235	1226	10.8
3.31	3.63	1240	1230	10.5
3.36	5.44	1255	1246	16.4
3.37	3.28	1255	1244	18.3
3.37	3.26	1271	1259	18.7
3.40	3.28	1272	1260	20.1
3.38	3.26	1277	1265	20.3
3.37	3.24	1282	1269	20.4
3.45	3.01	1303	1289	32.1
3.44	3.00	1309	1295	38.3
3.51	2.78	1341	1324	55.4
3.50	2.71	1349	1332	51.7
3.53	2.73	1356	1338	53.8
3.62	2.45	1423	1402	133
3.66	2.18	1439	1418	174
3.66	2.28	1444	1423	183
3.69	2.18	1462	1440	189
3.72	2.08	1478	1456	272
3.78	1.91	1518	1495	385
3.79	1.96	1528	1505	415

[a]Incident shock Mach number.

plot in Fig. 4 yields directly the second-order rate constant k_1 for Reaction (R1).

The results of this analysis are listed in Table II and the temperature dependence of the rate constants is shown in Fig. 5. The temperature T_m used in Fig. 5 is the mean of the frozen shock temperature (corresponding to zero reaction at $t=0$) and the temperature at the final point (e.g., Fig. 4) used in the determination of the rate constant. It is felt that this mean temperature is a more meaningful parameter than the frozen temperature because it accounts for the temperature variation due to the reaction.

A least squares fit to the data of Fig. 5 gives the Arrhenius equation

$$k_1(\text{cm}^3\,\text{mol}^{-1}\text{s}^{-1}) = 10^{16.61\pm0.13} \exp[(-48.0\pm0.8\,\text{kcal mol}^{-1})/RT], \quad (15)$$

where the error limits are standard errors. The 95% confidence limits for $\log_{10}A$ (cm^3 mol^{-1} s^{-1}) and E_a are ± 0.27 and ± 1.6 kcal mol^{-1}, respectively.

Two main criticisms may be directed at the above method. Firstly, the point by point adjustment for the temperature and density variations in the reaction zone is not consistent with the assumptions made in obtaining the integrated rate equation, Eq. (3), and may introduce an undetermined bias into the rate constant results. Secondly, the above method neglects the temperature dependence of the rate constant during the course of the endothermic reaction. However, as shown below, the use of these approximations is not serious in the case of high dilution.

In order to determine the effect of these approximations on the rate constants, a second method of data reduction was used. A computer program was written to calculate, by a least squares method, the Arrhenius parameters A and E_a which best fitted the experimental data. By this method, it was possible to explicitly account for the temperature variation of the rate constants throughout the reaction zone. The differential rate expression, Eq. (2), and Eqs. (4), (5), and (10)–(14) formed the basis of this program, together with the subroutine ZXSSQ (International Mathematical and Statistical Libraries, IMSL Library 3, 5th ed., 1975), which determined the minimum of the sum of squares. Input data consisted of the experimental conditions for each run ($T_{2,fz}$, $\rho_{21,fz}$, $[M]_1$, $[NF_3]_1$, and I_0) and the transmitted light intensity versus time data. The Arrhenius parameters which best fitted the experimental data were found to be $\log_{10}A$ (cm^3 mol^{-1} s^{-1}) = 16.79 and E_a = 49.1 kcal mol^{-1}.

A comparison of these Arrhenius parameters with those of Eq. (15) shows that the two methods of determining the rate constant yield comparable results. The experimental activation energies agree to within the experimental error, which justifies the approximate iterative method.

D. Comparison of rate constants

A summary of existing rate constant data for the dissociation of NF_3 is presented in Table III. For comparison purposes, the rate constants at 1100 and 1400 K are also shown.

Apart from the results of Dorko *et al.*[3] the rate con-

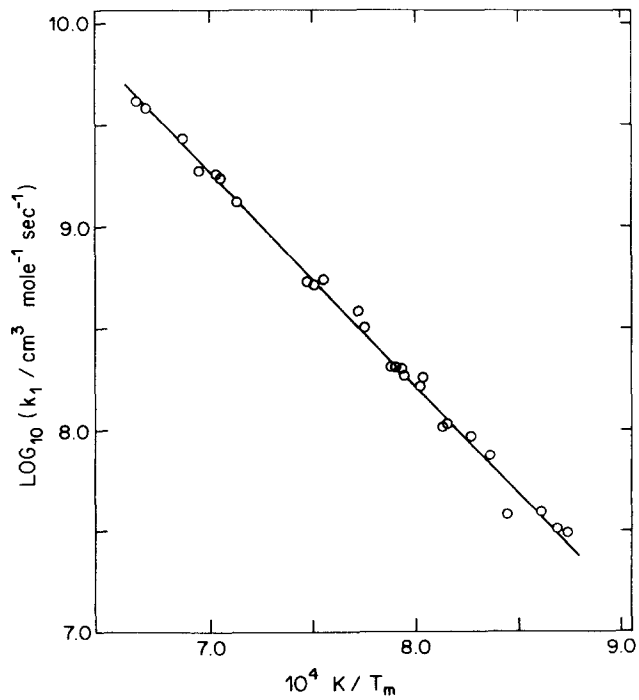

FIG. 5. Temperature dependence of the low pressure second-order rate constants k_1 for the dissociation of 1% NF_3 in argon.

TABLE III. Comparison of rate constants for dissociation of NF_3.

$\log_{10}A$ (cm^3 mol^{-1} s^{-1})	E_a (kcal mol^{-1})	k (cm^3 mol^{-1} s^{-1}) 1100 K	k (cm^3 mol^{-1} s^{-1}) 1400 K	Ref.
13.10 ± 0.02	30.1 ± 2.3	1.32×10^{7}	2.52×10^{8}	1
a	a	a	4.75×10^{8}	2
14.7[b]	56.3[b]	3.26×10^{3}	8.14×10^{5}	3
12.84[c]	38.6[c]	1.48×10^{5}	6.51×10^{6}	3
15.36	40.7	1.89×10^{7}	1.02×10^{9}	d
16.61 ± 0.13	48.0 ± 0.8	1.18×10^{7}	1.30×10^{9}	This work[e]
16.79	49.1	1.08×10^{7}	1.33×10^{9}	This work[f]

[a]Reference 2 gives only one numerical value of the rate constant at 1400 K.

[b]Arrhenius parameters for $k_{2nd\ order}$ obtained for representative data over the pressure range 0.8–60 atm. Notation is that used in Ref. 3.

[c]Estimated low pressure limit second-order rate constant k_a.

[d]Unpublished work of Breshears, Bird, and Schott cited in Ref. 3.

[e]Iterative method.

[f]Numerical integration method.

stants at 1000 and 1400 K are in reasonable agreement. At 1100 K, the rate constants from MT-R's[1] work and the present study are in good agreement. However at 1400 K, agreement between the two studies is relatively poor, and this is now attributed to an insufficiently fast detection system risetime. The effects of this deficiency become more pronounced in the rate constant measurements at higher temperatures.

The results of the present study and the unpublished work of Breshears, Bird, and Schott are in good agreement. However, a detailed comparison is not possible at the present time.

The rate constant data of Dorko *et al.*[3] differs significantly from the other data in Table III. The Arrhenius parameters for their $k_{2nd\ order}$ (third entry, Table III) have no significance, since the rate constant data span the entire falloff region (see Fig. 2, Ref. 3), and in the general pressure regime both k_{uni} and $k_{2nd\ order} = k_{uni}/[M]$ are functions of both temperature and pressure. The proximity of the value of the activation energy to $D(F_2N-F)$ must therefore be considered fortuitous and needs no further elaboration. From a series of plots of $1/k_{uni}$ vs $1/P$ at approximately the same temperature, Dorko *et al.* also obtained the low pressure limiting rate constant k_a (fourth entry, Table III), and by extrapolation to infinite pressure, the high pressure unimolecular rate constant, k^{∞}_{uni}. Within the framework of the simple Lindemann model this approach is legitimate, though for diagnostic purposes a plot of k_{uni} vs $1/P$,[13] or in the case of k^{∞}_{uni} an empirical plot of k_{uni} vs $P^{-1/2}$[14] would have been more appropriate. Moreover the scatter in the data (Fig. 4, Ref. 3) is such as to render the extrapolation of the limiting slope practically insignificant and is one possible reason for the very low preexponential factors for the limiting values of the rate constants k_a and $k^{\infty}_{uni} = 10^{11.3}\exp(-56\,500/RT)s^{-1}$. Such a low preexponential factor would require a large negative entropy of activation ($\Delta S^{\ddagger} = -12.6$ e.u.), whereas a negative $\Delta S^{\ddagger}$ for a simple bond fission reaction in the gas phase is physically impossible. It may be noted that the lowest theoretical A factor corresponding to an unrealistic tight activated complex for which $\Delta S^{\ddagger} = 0$ is given by $A = (ekT/h)\exp(\Delta S^{\ddagger}/R) = 10^{14.05}\,s^{-1}$ at 2000 K which is some three orders of magnitude higher than the reported value.[3]

Since these differences appeared to be too large to be attributed solely to experimental errors, and in view of the fact that in the temperature range of the study of Dorko *et al.* the product NF_2 radical is known to dissociate to NF + F,[15] an alternative explanation was sought. In several experiments in the temperature range 1650–1800 K, the ultraviolet absorption at 260 nm and infrared emission at 5.17 μ were monitored simultaneously. The results of one such experiment are presented in Fig. 6. It can be seen from this result that the two records vary in a similar manner throughout the relaxation zone. This indicates that the same species may be responsible for both the absorption and emission. Since the former is known to be due to the NF_2 radical, the infrared emission may result from a $2\nu_3$ transition of NF_2, which lies in the wavelength region monitored by both Dorko *et al.*[3] and in the present work. However, the above assignment, which is based on the observed ν_3 band of NF_2,[16,17] must be considered tentative because no observations of the overtone band of NF_2 appear to have been reported.

The above explanation of the ir emission signal is also consistent with the induction period observed by Dorko *et al.* in the temperature range 1500–1800 K. Since at lower temperatures the dissociation of NF_2 is slower, it is reasonable to expect a maximum to occur in the ir emission profile similar to that described in Ref. 3.

E. Comparison with theory

It is instructive to compare the experimental value of the activation energy with theoretical prediction. From the definition

$$-\frac{d\ln k_0^q}{d(1/RT)} = E_a^{\circ}(\text{theor}) \quad , \tag{16}$$

where k_0^q is the RRKM theory,[18] low pressure second-or-

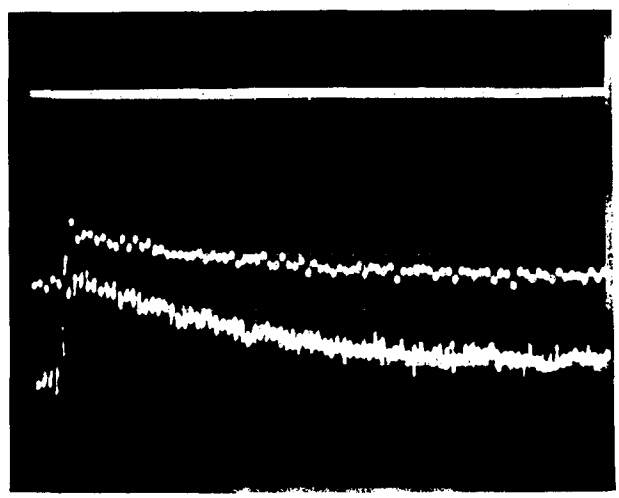

FIG. 6. Oscillogram of NF_2 absorption at 260 nm (lower trace) and infrared emission at 5.17 μ (upper trace); $p_1 = 40$ torr, $T_1 = 294$ K, $u_1 = 1290$ m s^{-1} and $T_2, T_2 = 1720$ K. Writing speed 20 μs div.$^{-1}$.

TABLE IV. Input parameters and energy contributions to the activation energy, E_a°(theor).

Molecular parameters		Ref.
E_0, kcal mol^{-1} [a]	57 ± 2	26
ω_i, cm^{-1} [b]	493(2), 647	27
	908(2), 1032	
E_z, kcal mol^{-1}	6.40	
s	6	
β [c]	0.9011	22
α_{NF_2}, cm^3 [d]	1.87×10^{-24}	
α_F, cm^3	0.47×10^{-24}	29
A_L, erg cm^6 [e]	38.62×10^{-60}	25
R_e, cm	$1.37_1 \times 10^{-8}$	27
Temperature dependent quantities at 1300 K		
a [f]	0.9836	22
$\langle\langle R_C^2 \rangle\rangle$, cm^2 [g]	10.224×10^{-16}	
ρ [g]	4.439	
W [g]	24.50_1	
$(s-1)/\gamma RT$, kcal mol^{-1} [g]	0.59_2	
$-E_{a,\mathrm{rot}}$, kcal mol^{-1} [h]	1.23	
$-\langle E_{\mathrm{n.e.}} \rangle$, kcal mol^{-1} [i]	2.2_0	
$(\langle \Delta E^2 \rangle)^{1/2}$, kcal mol^{-1} [j]	0.63_6	

[a] $E_0 \equiv D_0^\circ$ (NF_2–F).
[b] Vibrational frequencies for NF_3 molecule.
[c] Frequency dispersion parameter, $\beta = (s-1) \sum \omega_i^2/(\sum \omega_i)^2$.
[d] Polarizability of NF_2 estimated from atomic polarizabilities for F and N atoms, Ref. 28.
[e] Attraction constant for a London dispersion force, $A_L = [(3e\hbar/2m_e^{1/2})\alpha_1\alpha_2]/[(\alpha_1/N_1)^{1/2} + (\alpha_2/N_2)^{1/2}]$, where m_e is the electronic mass, subscripts 1 and 2 refer to F atom and NF_2 radical, and N is taken as the sum of outer shell electrons.
[f] Quantum correction factor to the zero point energy, $a = 1 - \beta \exp\{-2.419[(E_0 + \Delta E_J + E^\dagger)/E_z]^{1/4}\}$, where $\Delta E_j = -\rho RTl/2$, $E^\dagger = RT$, and $l = 2$.
[g] See text for definition.
[h] Calculated from Eq. (20).
[i] Calculated from Eq. (24).
[j] Calculated, see text.

der rate constant with more recent refinements,[19–24] we obtain the theoretical Arrhenius activation energy

$$E_a^\circ(\mathrm{theor}) = E_0 + \tfrac{3}{2}RT + (s-1)\gamma RT - RT\sum_{i=1}^{s}(H^0 - H_0^0)/RT + E_{a,\mathrm{rot}} + \langle E_{\mathrm{n.e.}} \rangle \quad . \tag{17}$$

In Eq. (17), E_0 is the critical energy, s is the *total* number of vibrational degrees of freedom, $\sum(H^0 - H_0^0)/RT$ denotes the corresponding harmonic oscillator functions, $E_{a,\mathrm{rot}}$ is the rotational contribution to the activation energy from the centrifugal correction,[19] $\langle E_{\mathrm{n.e.}} \rangle$ is the possible contribution at low pressures from the nonequilibrium weak collision correction,[20,21] and γ reflects contributions from higher order terms in the rate constant,[5]

$$\gamma = W^{-1} + (n-2)W^{-2} + (n^2 - 6n + 6)W^{-3} + \cdots \quad , \tag{18}$$

$$W = (E_0 + a\,E_z)/RT \quad , \tag{19}$$

where $n = s - 1$; $E_z (= \frac{1}{2}\sum hc\omega_i)$ is the zero point energy and a is a quantum correction factor.[22,23]

The centrifugal contribution to the Arrhenius activation energy has been derived by Waage and Rabinovitch[19] as

$$E_{a,\mathrm{rot}} = -n\rho RT/(W + n\rho) \quad , \tag{20}$$

$$\rho = (I^\dagger/I) - 1 \quad , \tag{21}$$

where $I^\dagger/I$ is the ratio of the principal moments of inertia for adiabatic rotations for activated complex and molecule. An alternate approximation for $E_{a,\mathrm{rot}}$ due to Hay and Belford[24] gives $E_{a,\mathrm{rot}} = -n\rho RTW/(W+1)^2 \approx -n\rho RT/(W+1)$. If molecule and complex are treated as a quasi-diatomic species, $I^\dagger/I = \langle\langle R_c^2 \rangle\rangle/R_e^2$, where R_e is the equilibrium internuclear distance in the molecule (i.e., the NF_2–F bond length) and $\langle\langle R_c^2 \rangle\rangle$ is the corresponding *apparent* square of the distance[19(b)] in the complex. For a London dispersion force between two particles[19(b)]

$$\langle\langle R_c^2 \rangle\rangle = 1.354(2A_L/kT)^{1/3} \quad , \tag{22}$$

where A_L can be evaluated[25] from polarizability data.

Troe and Wagner[20,21] have shown that for an exponential model of collisional transition probability the rate expression contains a collision efficiency factor $P_{\Delta E^2} = (1 + RT/\alpha_E)^{-2}$, which corrects for nonequilibrium effects and departures from the strong collision assumption, where $\alpha_E^2 = \langle \Delta E^2 \rangle/2$ and $\langle \Delta E^2 \rangle$ is the mean squared energy transferred per collision. It has been further shown[20,21] that $\langle \Delta E^2 \rangle^{1/2} \propto T^{1/2}$, hence we obtain a contribution to the Arrhenius activation energy

$$\langle E_{\mathrm{n.e.}} \rangle = -\frac{RT}{1 + \langle \Delta E^2 \rangle^{1/2}/\sqrt{2}RT} \quad . \tag{23}$$

The necessary input data and the contributions to the activation energy are collected in Table IV. The activation energy in kcal mol^{-1} evaluated from Eq. (17) at 1300 K is

$$E_a^\circ(\mathrm{theor}) = 50.2 + \langle E_{\mathrm{n.e.}} \rangle \quad , \tag{24}$$

using the Waage and Rabinovitch[19] formulation for the centrifugal contribution. The expresssion for $E_{a,\mathrm{rot}}$ of Hay and Belford leads to $E_a^\circ(\mathrm{theor}) = 49.3 + \langle E_{\mathrm{n.e.}} \rangle$, and both formulations lead to gratifying agreement with the observed activation energy of 48.0 ± 0.8 kcal mol^{-1}, since $\langle E_{\mathrm{n.e.}} \rangle$ provides a negative contribution, Eq. (23).

From Eq. (23) we note that for $(\langle \Delta E^2 \rangle)^{1/2} \gg RT$, $\langle E_{\mathrm{n.e.}} \rangle = -\sqrt{2}\,(RT)^2/(\langle \Delta E^2 \rangle)^{1/2}$, which corresponds to the strong collision limit. For $\langle \Delta E^2 \rangle^{1/2} \ll RT$, we obtain in the "weak collision limit" $\langle E_{\mathrm{n.e.}} \rangle = -RT$, which is a maximum negative contribution to the activation energy (~2.6 kcal at 1300 K). An estimate for $\langle \Delta E^2 \rangle^{1/2}$ can be obtained from Eq. (24) by equating E_a°(theor) $= E_a^\circ$(obs) $= 48.0 \pm 0.8$ kcal mol^{-1}. We thus obtain $\langle \Delta E^2 \rangle^{1/2} = 0.64$ kcal mol^{-1} $= 0.245\,RT$ at 1300 K, a most reasonable value.

The observed preexponential factor for NF_3 decomposition of $\log A$ cm^3 mol^{-1} s^{-1} $= 16.61$ is in line with other high temperature studies of four and five atom molecules such as NH_3 [$\log A$(cm^3 mol^{-1} s^{-1}) $= 16.39$],[20] $(CN)_2$(16.60),[20] NO_2Cl (16.46),[20] H_2O_2 (16.67),[20] and CH_4 (17.3).[30]

ACKNOWLEDGMENTS

The support of the National Research Council and the Defence Research Board, Canada, are gratefully acknowledged. The authors also wish to thank Dr. R.

Yamdagni for the mass spectrometric analyses and Dr. H. Wieser for several helpful discussions.

*Postdoctoral Fellow.

[1]K. O. MacFadden and E. Tschuikow-Roux, J. Phys. Chem. 77, 1475 (1973); hereafter referred to as MT-R.
[2]G. L. Schott, L. S. Blair, and J. D. Morgan, Jr., J. Phys. Chem. 77, 2823 (1973).
[3]E. A. Dorko, U. W. Grimm, K. Scheller, and G. W. Mueller, J. Chem. Phys. 63, 3596 (1975).
[4]A. Kennedy and C. B. Colburn, J. Chem. Phys. 35, 1892 (1961).
[5]E. Tschuikow-Roux, K. O. MacFadden, K. H. Jung, and D. A. Armstrong, J. Phys. Chem. 77, 734 (1973).
[6](a) F. A. Johnson and C. B. Colburn, J. Am. Chem. Soc. 83, 3043 (1961); (b) C. B. Colburn (private communication, 1976).
[7]S. Gordon and B. J. McBride, NASA Spec. Publ. **SP-273** (1971).
[8]D. R. Stull and H. Prophet, Natl. Stand. Ref. Data Ser., Natl. Bur. Stand. 37, (1971).
[9]L. M. Brown and B. de B. Darwent, J. Chem. Phys. 42, 2158 (1965).
[10]A. P. Modica and D. F. Hornig, J. Chem. Phys. **49**, 629 (1968).
[11]M. A. A. Clyne and J. Connor, J. Chem. Soc. Faraday Trans. II 68, 1220 (1972).
[12]T. A. Jacobs and R. R. Giedt, J. Quant. Spectrosc. Radia. Transfer 3, 289 (1963).
[13]H. S. Johnston, J. Chem. Phys. 20, 1103 (1952).
[14]B. S. Rabinovitch and K. W. Michel, J. Am. Chem. Soc. 81, 5065 (1959).
[15]A. P. Modica and D. F. Hornig, J. Chem. Phys. 43, 2739 (1965).
[16]M. D. Harmony and R. J. Myers, J. Chem. Phys. 37, 636 (1962).
[17]M. E. Jacox, D. E. Milligan, W. A. Guillory, and J. J. Smith, J. Mol. Spectrosc. 52, 322 (1974).
[18](a) R. A. Marcus, J. Chem. Phys. 20, 359 (1952); 43, 2658 (1965); (b) G. M. Wieder and R. A. Marcus, *ibid.* 37, 1835 (1962).
[19](a) E. V. Waage and B. S. Rabinovitch, J. Chem. Phys. 52, 5581 (1970); (b) Chem. Rev. 70, 377 (1970).
[20]J. Troe and H. Gg. Wagner, Ber. Bunsenges. Phys. Chem. 71, 937 (1967).
[21]J. Troe and H. Gg. Wagner, in *Physical Chemistry of Fast Reactions*, edited by B. P. Levitt (Plenum, New York 1973), Vol. I.
[22]G. Z. Whitten and B. S. Rabinovitch, J. Chem. Phys. 38, 2466 (1963); 41, 1883 (1964).
[23]D. C. Tardy, B. S. Rabinovitch, and G. Z. Whitten, J. Chem. Phys. 48, 1427 (1968).
[24]A. J. Hay and R. L. Belford, J. Chem. Phys. 47, 3944 (1967).
[25]E. Tschuikow-Roux, J. Phys. Chem. 72, 1009 (1968).
[26]B. de B. Darwent, Natl. Stand. Ref. Data Ser., Natl. Bur. Stand. 31 (1970).
[27]R. J. L. Popplewell, F. N. Masri, and H. W. Thompson, Spectrochim. Acta 23, 2797 (1967).
[28]J. A. A. Ketelaar, *Chemical Constitution* (Elsevier, New York, 1958).
[29]W. J. Stevens and F. P. Billingsley, Phys. Rev. A 8, 2236 (1973).
[30]R. Hartig, J. Troe, and H. Gg. Wagner, Thirteenth Symp. (Int.) Combust. [Proc.], 147 (1971).

Shock tube decomposition of dilute mixtures of nitrogen trifluoride in argon

Cite as: J. Chem. Phys. **63**, 3596 (1975); https://doi.org/10.1063/1.431750
Published Online: 03 September 2008

Ernest A. Dorko, U. W. Grimm, K. Scheller, and Gerhard W. Mueller

Shock tube decomposition of dilute mixtures of nitrogen trifluoride in argon

Ernest A. Dorko

Department of Aero-Mechanical Engineering, Air Force Institute of Technology, Wright-Patterson Air Force Base, Ohio 45433

U. W. Grimm and K. Scheller

Chemistry Research Laboratory, Aerospace Research Laboratories, Wright-Patterson Air Force Base, Ohio 45433

Gerhard W. Mueller

Universal Energy Systems, Inc., Wright-Patterson Air Force Base, Ohio 45433
(Received 3 April 1975)

The decomposition of 0.25%, 0.50%, and 1.00% NF_3 in argon was studied in a reflected shock wave. In these dilute mixtures the unimolecular decomposition pathway can be studied independently of other modes of decomposition. The temperature range of the study was 1500–2400°K and the total pressure range was 0.8–60 atm. The total gas concentration behind the reflected shock ranged from 5×10^{-6} to 3.6×10^{-4} mol/cc. Kinetic measurements were made by following the decay of emission of the $\nu_3+\nu_1$ combination band of NF_3 at 5.18 μ. The unimolecular rate constants of the Lindemann mechanism were obtained from the emission decay data and were converted to second order rate constants by dividing by the total gas concentration. The Arrhenius parameters calculated by a least squares analysis of the second order rate constants are given as $k = 10^{14.7}\exp(-56300/RT)$ cc/mol sec. The activation energy for the reaction is very close to the first N–F bond energy of 57 kcal/mol. Calculations using the Slater integral were in good agreement with experimental results. The results suggest that under the reported conditions vibrational equilibrium is not maintained during reaction.

INTRODUCTION

In a continuing effort to separate the unimolecular decompositions of molecules from the other pathways for decomposition which they often exhibit a study was conducted on dilute mixtures of nitrogen trifluoride (NF_3) in argon. A shock tube was used to cause the decomposition to occur and the observance of the decay of intensity of the infrared emission from NF_3 was used to determine the kinetics of the decomposition. This technique has been used previously to study similar decompositions.[1,2]

A recent study of the shock induced decomposition of NF_3[3] has been reported by MacFadden and Tschuikow-Roux (MT-R). They performed an analysis on the assumed equilibrium

$$NF_3 + M \underset{k_{-M}}{\overset{k_M}{\rightleftarrows}} NF_2 + F + M. \qquad (1)$$

They were able to establish an approximate first order dependence of the decomposition on argon. They also reported an Arrhenius expression for k_M. Their expression is puzzling, however, because the activation energy (30.1 ± 2.3 kcal/mol) is lower (for their experimental conditions) by a factor of about $10RT$ than the bond energy reported by Kennedy and Colburn[4] for the first NF bond (57.1 ± 2.5 kcal/mol).

The present report details the analysis of this system assuming a unimolecular decomposition according to the Lindemann mechanism.[5]

EXPERIMENTAL SECTION

The stainless steel shock tube employed has been described elsewhere.[1] The test gas mixtures ranged from 0.25% to 1% NF_3 (97.5%) in argon (99.999%). The gas mixtures were prepared in stainless steel containers. Kinetic measurements were made for the reaction occurring behind the reflected shock by means of infrared emission measurements.[1] For this purpose CaF_2 windows were placed in the flat wall of the shock tube 12 mm from the end flange of the driven section. Shock parameters were calculated for the specific gas mixtures from the initial shock velocity assuming frozen chemistry. Heat capacities for NF_3 were obtained from the JANAF tables.[6] The total gas concentration behind the reflected shock ranged from 5×10^{-6} to 3.6×10^{-4} mol/cc. The temperature range was 1500–2400 °K and the total pressure range was 0.8–60 atm. A total of five hundred shocks were used in the analysis.

The emission from the shock tube was focused by means of a CaF_2 lens system onto an infrared detector. A filter was placed in the beam prior to its entry into the detector. An interference filter transmitting at 5.25 μ (half-bandpass width of 0.7 μ) was used in conjunction with an indium antimonide detector (Barnes Engineering) cooled with liquid nitrogen. Nitrogen trifluoride has a combination band ($\nu_3+\nu_1$) at 5.18 μ.[7] Neither the NF_2 nor N_2F_4 exhibit any absorption bands in this region of the spectrum.[8] This band was used for the kinetic studies. The signal from the IR detector was fed through an impedance matched preamplifier (Perry Associates) into an oscilloscope (Tetronix model 555), which was triggered by the heat gauge at the last velocity station. A time mark generator was used to determine time on the oscillogram. The curves obtained on the oscilloscope traces exhibited the expected decay at temperatures above 1800 °K. Below this temperature

an induction period was observed. The induction period is characterized by a maximum in the emission curve. This portion of the curve is followed by the exponential decay portion, which is expected for simple, unimolecular reactions. The induction period ranged from a few μsec up to about 30–40 μsec. This phenomenon has been observed previously for other systems.[9,10]

The oscillograms were reduced by plotting the logarithm of the intensity versus time. These plots produced straight line portions for the first 15%–25% of the curve for the total observation time after the induction period. Rate constants were calculated from the slopes of the straight line portions. These constants were designated k_{uni}. Total and NF_3 gas concentrations were calculated at reflected shock conditions under the assumption that the gases were ideal.

RESULTS AND DISCUSSION

The Lindemann mechanism for the system under study is

$$NF_3 + M \underset{k_d}{\overset{k_a}{\rightleftharpoons}} NF_3^* + M, \tag{2}$$

$$NF_3^* \overset{k_e}{\rightarrow} NF_2 + F. \tag{3}$$

The rate expression for the decomposition of NF_3 assuming this mechanism is

$$-\frac{d[NF_3]}{dt} = \frac{k_a k_e [M][NF_3]}{k_d[M] + k_e}, \tag{4}$$

where k_a, k_d, and k_e are the rate constants for activation, deactivation, and decomposition, respectively, and [M] and $[NF_3]$ represent total and nitrogen trifluoride concentrations, respectively, in mol/cc.

In order to establish the validity of this analysis for the data obtained in the present case it must first be shown that at a given constant [M] a plot of $\log[NF_3]$ versus time produces a straight line. This was shown to be true for the first 15%–25% of reaction for all of the data reduced. After this initial reaction period, most likely the reverse reaction begins to play a significant role in the reaction scheme; and also the interaction of NF_3 with reaction products may become important.[3] In any event the log plots begin to deviate from a single, straight line. In addition to this first consideration, in order to preclude the interference of a reaction for decomposition which is bimolecular in NF_3 it must be shown that there is no dependence of k_{uni} on the NF_3 concentration. Figure 1 shows an Arrhenius plot of data of k_{uni}. The upper line represents the best straight line fit of data obtained under conditions of constant [M] with a variation in $[NF_3]$ of a factor of 4. The data show that k_{uni} is not dependent on $[NF_3]$.

In contrast to this result, the concentration dependence of k_{uni} on [M] can be seen by a comparison of the two lines. The ratio of total gas concentrations for the data is 6.8. The best straight line fits of the two data sets produced the result that the data points are separated by a factor of 5.5. From a comparison of these two numbers the decomposition rate is shown to have a power dependence on [M] of 0.84. This result is similar to that found by MT-R.[3] For the conditions of their experiment they obtained a total gas concentration dependence of 0.93.

The slight discrepancy between the two numbers is not surprising since conditions are different. MT-R reported experiments in a lower pressure regime (2.7–6.0 atm),[3] in which the reaction is closer to the bimolecular region. In the present experiments the smaller concentration dependence [M] indicates that the reaction is being observed closer to the high pressure (first-order) region. From these results, then, it is clear that within the scatter band of the shock tube analysis the rate is independent of $[NF_3]$ and dependent on [M].

It is to be noted, however, that the analysis assuming the Lindemann mechanism can only be approximate in the present case. Since at the lower temperatures an induction period was observed on the oscilloscope trace, it is known that the reaction proceeds by a mechanism more complex than that postulated for the simple mechanism. The nature of the induction period is not yet completely clear. However, there is evidence to suggest that a low lying vibrational state of the molecule can serve as an intermediate in unimolecular shock tube reactions.[1,10] Since in the present case the induction period was only detectable at the lower temperatures, and even then, for a relatively short period of the reaction time, it is felt that such a simple analysis is justified.

The rate constants were converted into second order rate constants ($k_{2nd\ order}$) by dividing each by [M]. Representative results are displayed in Fig. 2. The Arrhenius parameters calculated by a least squares analysis of the data are

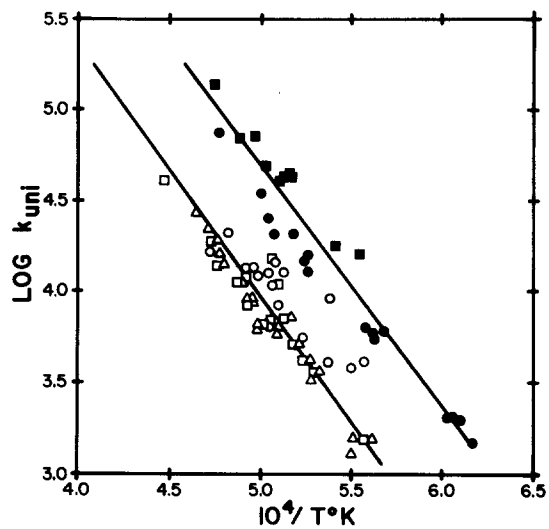

FIG. 1. A plot of $\log k_{uni}$ vs $1/T$°K. The upper line represents the best straight line fit of data taken at a total gas concentration of 19×10^{-6} mol/cc (± 10%) for 0.25% NF_3 (○), 0.50% NF_3 (□) and 1.00% NF_3 (△). The lower line represents the best straight line fit of data taken at a total gas concentration of 130×10^{-6} mol/cc (±10%) for 0.25% NF_3 (■) and for 1.00% NF_3 (●). The separation between lines is 0.74 log units. This separation corresponds to an argon power dependence of 0.84.

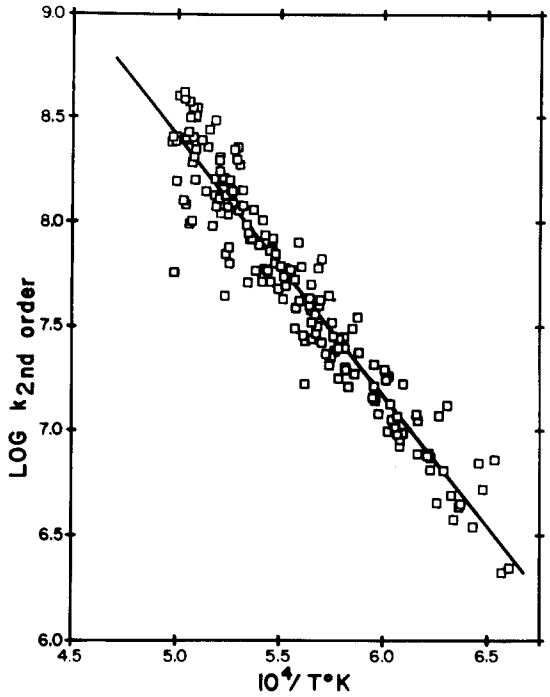

FIG. 2. An Arrhenius plot of representative data for $k_{\text{2nd order}}$ for the pressure range 0.8–60 atm. (The units of the rate constant are cc/mol · sec.)

$$k_{\text{2nd order}} = 10^{14.7} e^{-56\,300/RT}\ \text{cc/mol} \cdot \text{sec}. \tag{5}$$

The activation energy is encouragingly close to the bond energy of the first NF bond[4] and the frequency factor is within the expected range for a bimolecular reaction.[11] These results are, however, substantially different from those reported by MT-R.[3] In order to test for the reasonableness of the present results using the assumption of the Lindemann mechanism a further treatment of the data was performed in order to determine the rate constants in the high and low pressure regions.

The data were analyzed in two different ways. Initially a series of plots of $\log k_{\text{uni}}$ vs $\log p$[12] were prepared for selected shock results obtained at the same temperature. Figure 3 shows a typical plot. The data are clearly in

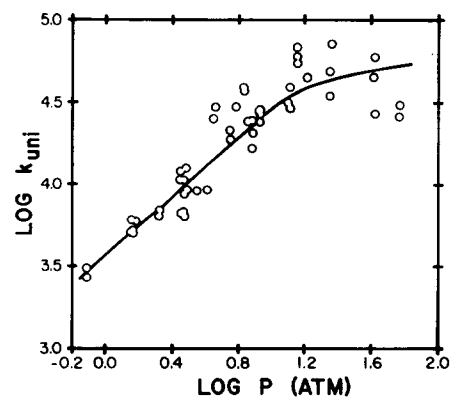

FIG. 3. A plot of $\log k_{\text{uni}}$ vs $\log P_5$ obtained at 2000 ± 20 °K. The straight line portion of the curve is the best straight line fit of the data with slope unity. The bend in the curve occurs near 10 atm.

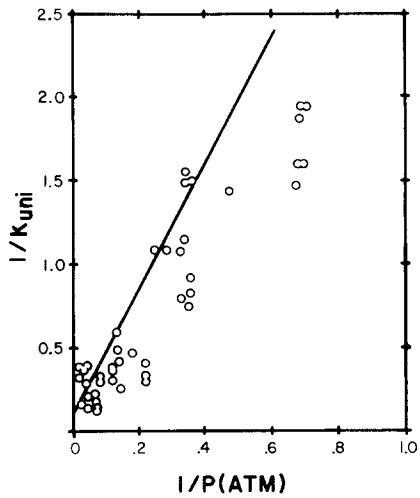

FIG. 4. A plot of $1/k_{\text{uni}}$ vs $1/P_5$ obtained at 2000 ± 20 °K.

the fall-off region. At the lower pressures a straight line of slope unity provides an approximate fit of the data. This result is consistent with the Lindemann mechanism.[12] At pressures near 10 atm, k_{uni} becomes less dependent on pressure and the increasing slope of the curve becomes very evident. However, the k_{uni} has not become independent of pressure even at the maximum pressure of the study which was 60 atm. This result is as expected for a molecule with 4 or 5 oscillators.[12]

Since the experiments were performed in the fall-off region a quantitative analysis of the data was made on a series of plots of $1/k_{\text{uni}}$ vs $1/P$[12] for selected shock results obtained at the same temperature. Representative results are shown in Fig. 4. The straight line was drawn in such a way as to give the best fit through the points in the high pressure region (i.e., at the limit of the data points). In this way the line corresponds to the line of limiting slope.[12] This procedure allows a determination of k_a and of $k_{\text{uni}(P=\infty)}$ (equivalent to $k_a k_e/k_d$). The procedure seems to be valid only when applied to the fall-off region. From the limiting slope of the line through the data points at high pressure k_a can be estimated, and from the intercept of the line it is possible to estimate $k_{\text{uni}(P=\infty)}$. Equations (6) and (7) give the Arrhenius parameters which were determined by reducing the results of a series of such plots.

$$k_a = 10^{12.84} e^{-38\,600/RT}\ \text{cc/mol} \cdot \text{sec}, \tag{6}$$

$$k_{\text{uni}(P=\infty)} = 10^{11.3} e^{-56\,500/RT}\ \text{sec}^{-1}. \tag{7}$$

These results must be taken to be reasonable estimates of the high and low pressure rate constants since the exact analytical function to correlate the data could not be determined. It is to be noted, however, that the high pressure activation energy is very close to the bond strength of the initial NF bond.[4] Also the decrease in activation energy from the high to the low pressure value (17.9 kcal/mole) corresponds to a decrease of about $4RT$ in the temperature range under consideration. This decrease is as expected from the simple Hinshelwood–Lindemann theory $[E_\infty - E_0 = (S-1)RT]$.[12]

The frequency factors in both cases are somewhat lower than expected for the corresponding uni- or bimolecular values. Since in the Lindemann mechanism the high pressure rate constant is a composite of three rate constants this result is not disturbing. However, for the low pressure results it is felt that the value is somewhat low.

A comparison of present results with previous results is instructive. Two determinations of the low pressure rate constants have been made. MT-R[3] obtained the Arrhenius expression

$$k = 10^{13.1}\, e^{-30\,100/RT}\ \text{cc/mol} \cdot \text{sec}. \tag{8}$$

As previously noted the activation energy seems too low even if allowance is made for the inadequacy of the simple Lindemann mechanism in predicting the difference between high and low pressure activation energies. Since their lowest pressure was 2.7 atm, most likely they were not entirely in the low pressure regime. Indeed the dependence on [M], reported as 0.93, indicates that this was the case.

In a more recent study Breshears, Bird, and Schott[13] obtained an expression for the low pressure Arrhenius equation which is shown as

$$k = 2.31\times10^{15}\, e^{-40\,700/RT}\ \text{cc/mol} \cdot \text{sec}. \tag{9}$$

This equation was determined over the temperature range 1300–2200 °K for a pressure range of 0.1–0.5 atm. The difference between high and low pressure activation energies corresponds to about $4RT$. This difference is in good agreement with the simple theory. The present results correspond to this value of the low pressure activation energy within experimental error. However, it must be noted that there is a significant difference between the frequency factors in the two cases.

NUMERICAL ANALYSIS

In order to further test the reasonableness of the values obtained under the assumption of a unimolecular decomposition, calculations of the rate constants were attempted by the use of the Kassel[14] integral (the classical RRK approach),[12] the Slater integral,[14] and by a modified RRKM approach.[12]

The Kassel integral proved to be quite inadequate for the task of calculating reasonable rate constants since it underestimated the experimental constants by several orders of magnitude. This observation has been made previously in connection with other unimolecular decompositions.[15] In addition, the shape of the calculated curve was so significantly different from the experimental curve that it precluded the use of a parametric approach toward convergence.

A modified RRKM approach was used in order to overcome somewhat the limitations of the Kassel method. The approach taken is similar to the method developed by Bunker.[12,16,17] The three terms which must be evaluated are the collisional frequency ω, the rate constant for decomposition k_E, and the probability that a molecule will have sufficient energy to react $P(E)\,dE$.

Collisional frequency was calculated as a product of the collision number Z (obtained by kinetic gas theory with no repulsive potential) and the reacting gas concentration [M]. The collision is assumed between NF_3 and argon. The cross sectional diameter for collision was taken to be 3.1 Å. The expression for Z is

$$Z = 5.233\times10^{12}T^{1/2}\ \text{cc/mol} \cdot \text{sec}. \tag{10}$$

The expression utilized for k_E is

$$k_E = \left(\frac{Q_{r^+}}{Q_r}\right)\left(\frac{\Pi_i^S \nu_i}{\Pi_i^{S-1}\nu_{i^+}}\right)\left(\frac{E-E_c+E_{Z^+}^{S-1}}{E+E_Z}\right). \tag{11}$$

If it is assumed that the rotational levels do not change during the activation process then the ratio of partition functions (Q_{r^+}/Q_r) becomes the ratio of the square roots of the products of the moments of inertia. The molecular dimensions for the ground state molecule were obtained from a report by Schomaker and Lu.[18] It was assumed that the reacting NF bond length had increased in the transition state from 1.37 to 1.67 Å. Based on this assumption the ratio of the rotational partition functions was calculated to be 1.29.

In order to determine the ratio of vibrational fundamentals the data of Popplewell, Masri, and Thompson[19] on the vibrational fundamentals of NF_3 were used for the ground state. It was assumed that the vibration due to the NF stretch (ν_1) becomes the reaction coordinate. It was further assumed that in the transition state the degeneracy of ν_3 and ν_4 is destroyed and that the two degenerate vibrations are split by 200 cm^{-1}. The fundamental ν_2 remains unchanged. It is felt that these assumptions provide a reasonable estimate of the desired ratio. The final result for the ratio of vibrational fundamentals is 3.266×10^{13} sec^{-1}. The ground state energies E_{Z^+} and E_Z were calculated to be 4929 and 6403 cal/mol, respectively. E_c was taken to be 57 kcal/mol, the value accepted for the bond strength of the first NF bond.[4] On multiplying together the ratios for rotation and vibration and designating the product as D, a value for D of 4.213×10^{13} sec^{-1} was obtained. The expression used for the energy probability is the usual one developed by RRK for a classical model[12,16,17] and will not be repeated here.

The final nondimensionalized equation is shown by

$$k_{\text{uni}} = \frac{D}{(S-1)!}\int_b^\infty \frac{X^{S-1}e^{-X}\left(\dfrac{X-b+c}{X+e}\right)^{S-1}dX}{1+\dfrac{D}{Z[\text{M}]}\left(\dfrac{X-b+c}{X+e}\right)^{S-1}}, \tag{12}$$

where $X = E/RT$, $b = E_c/RT$, $C = E_{Z^+}/RT$, and $e = E_Z/RT$. The value of [M] was calculated as (0.01) P/RT. The factor 0.01 was included in order to correct for the fact that only about 1% of the actual collisions which occur are between NF_3 and argon.

Equation (15) was solved by means of a numerical integration using program KUNI written for a CDC 6600 computer.[20] A plot of $\log k_{\text{uni}}$ vs $\log P$ at 2000 °K based on the results of these calculations is presented as part of Fig. 5. A parametric approach was used in order to produce the best fit of the calculated curve to the data. The value of s was varied from 6 (the value required by the RRKM approach) to 2. The closest fit occurred

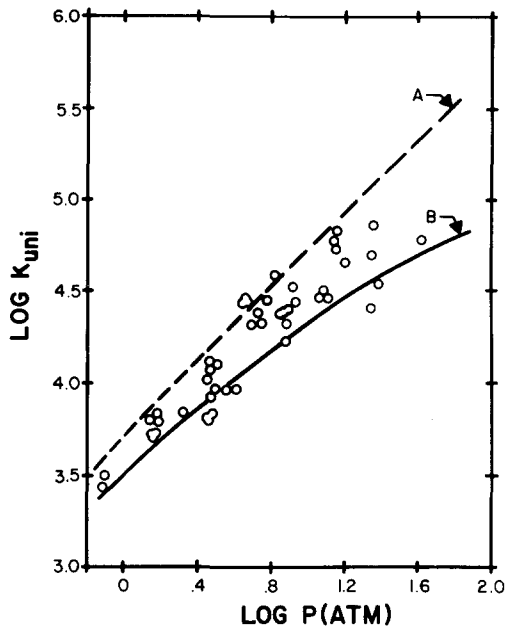

FIG. 5. Dependence of rate constant on pressure. Curve A is a plot of calculations based on the RRKM approach. Curve B is a plot of calculations based on the Slater integral. The points (o) are for the data taken at 2000 ± 20 °K.

when s was taken as 4. This is the curve shown in Fig. 5. The shape of the curve, however, was not appreciably altered by this procedure. On comparison of the calculated results with the experimental points, it is immediately evident that while the calculated rate constants are of the right order of magnitude and give a reasonable estimate of the experimental rate constants at lower pressures, the calculated curve does not correctly reproduce the lessened pressure dependence of the experimental data points at higher pressure.

The final approach taken utilized the Slater integral[14,21] in order to calculate the theoretical rate constant curve. The nondimensionalized equation used is[14]

$$\frac{k}{k_\infty}=\frac{1}{\Gamma[(n+1)/2]}\int_0^\infty \frac{X^{1/2}(n-1)\,e^{-X}\,dX}{1+(X^{(1/2)(n-1)}/\theta)}\,, \tag{13}$$

where $X=(E-E_a)/RT$ and n = the number of nongenerate vibrational modes in the molecule (taken to be 4 for NF_3). A simplified, though reasonable, estimate of θ was taken as

$$\theta=\frac{10Z[\mathrm{M}]}{A}\,b^{1/2(n-1)}\,, \tag{14}$$

where A is the high pressure Arrhenius frequency factor, Z is the collision number, [M] is the gas concentration, and $b=E_a/RT$. The values for E_a and A were taken to be the experimentally determined high pressure Arrhenius parameters, 56.5 kcal/mol and $10^{11.3}$ sec^{-1}, respectively. Z and [M] were calculated as previously discussed. The factor 10 was included in order to give the closest correspondence between the calculated and experimental values for the rate constants. This technique has been used previously with the Slater integral.[14]

The numerical integration to solve Eq. (14) was performed with program KUNI.[20] A representative plot of $\log k_{uni}$ vs $\log P$ at 2000 °K is included in Fig. 5. The coincidence of the calculated curve with the experimental data points is excellent. Of course it must be borne in mind that a parameter was added to insure this result. The most significant correspondence is the correct reproduction by the calculation of the bend in the data points at higher pressure.

Based on the results presented it can be seen that a good estimate of the actual rate constant can be obtained by using the Slater integral in the parametric form presented as Eq. (13). It is somewhat puzzling that a calculation based on the modified RRKM approach should correspond less well than a calculation based on the Slater approach for a situation involving equilibrium heating. It is tentatively suggested that in the present experiment, vibrational equilibrium is not being maintained. Some evidence to support this suggestion was presented in the experimental section. The presence of an induction region at the lower temperatures suggests that NF_3 decomposition under present conditions is proceeding similarly to other systems where this vibrational nonequilibrium has been reported.[10] Even in the region where the induction period is not evident under experimental conditions, the theoretical analysis suggests that vibrational equilibrium is not being maintained. This means that the Slater approach, based as it is on vibrational nonequilibrium, is a more adequate model in the present case. However, it must be considered that arguments based on the classical models employed in the present analysis must ultimately be verified by a strict quantum mechanical analysis. In the meantime it is recommended that calculations to estimate k_{uni} under any desired conditions of temperature and pressure should be performed with the Slater integral.

ACKNOWLEDGMENTS

The authors wish to thank W. D. Breshears, P. F. Bird, and G. L. Schott for the use of their experimental results prior to publication. They would also like to thank C. B. Colburn for helpful discussions during the course of this work. One of us (GWM) would like to acknowledge sponsorship of this research by the Air Force Aerospace Research Laboratories, Air Force Systems Command, United States Air Force under Contract No. F33615-74-C-4006.

[1] E. A. Dorko, R. W. Crossley, U. W. Grimm, G. W. Mueller, and K. Scheller, J. Phys. Chem. 77, 143 (1973).
[2] E. A. Dorko, U. W. Grimm, K. Scheller, and G. W. Mueller, J. Phys. Chem. (submitted for publication).
[3] K. O. MacFadden and E. Tschuikow-Roux, J. Phys. Chem. 77, 1475 (1973).
[4] A. Kennedy and C. B. Colburn, J. Chem. Phys. 35, 1892 (1961).
[5] F. A. Lindemann, Trans. Faraday Soc. 17, 598 (1922).
[6] D. R. Stull and H. Prophet (eds.), Nat. Stand. Ref. Data Ser., Nat. Bur. Stand. 37 (1971).
[7] E. L. Pace and L. Pierce, J. Chem. Phys. 23, 1248 (1955).
[8] M. D. Harmony and R. J. Myers, J. Chem. Phys. 37, 636 (1962).
[9] J. P. Appleton, M. Steinberg, and D. J. Liguarnik, J. Chem. Phys. 52, 2205 (1970).

[10]E. A. Dorko, D. B. McGhee, C. E. Painter, A. J. Caponecchi, and R. W. Crossley, J. Phys. Chem. **75**, 2526 (1971).
[11]A. A. Frost and R. G. Pearson, in *Kinetics and Mechanism*, 2nd ed. (Wiley, New York, 1961), p. 75.
[12]R. E. Weston, Jr., and H. A. Schwarz, in *Chemical Kinetics* (Prentice-Hall, Englewood Cliffs, 1972), Chap. 5.
[13]W. D. Breshears, P. F. Bird, and G. L. Schott (private communication).
[14]H. O. Pritchard, R. G. Saunders, and A. F. Trotman-Dickenson, Proc. R. Soc. A 217, 563 (1958).
[15]G. B. Skinner, in *Introduction to Chemical Kinetics* (Academic, New York, 1974), p. 75.
[16]D. L. Bunker, in *Theory of Elementary Gas Reaction Rates* (Pergamon, Oxford, 1966), Chap. 3.
[17]E. A. Dorko, U. W. Grimm, G. W. Mueller, and K. Scheller, "The Shock Tube Isomerization of Cyclopropane with Infrared Analysis," Aerospace Research Laboratories, Report No. ARL-71-0089, Wright-Patterson Air Force Base, OH 45433, 1971.
[18]V. Schomaker and C. Lu, J. Am. Chem. Soc. **72**, 1182 (1950).
[19]J. L. Popplewell, F. N. Masri, and H. W. Thompson, Spectrochim Acta, A **23**, 2797 (1967).
[20]G. W. Mueller and E. A. Dorko, Program kuni, QCPE No. 282, Quantum Chemistry Program Exchange, Chemistry Department, Indiana University, Bloomington, IN.
[21]N. B. Slater, Philos. Trans. R. Soc. London, Ser. A **246**, 57 (1953).

NF_3 decomposition behind shock waves

V.M. Doroshchenko, N.N. Kudriavtsev, A.M. Sukhov and D.P. Shamshev
Moscow Institute of Physics and Technology, Dolgoprudny, Moscow Region 141700, Russia

Received 6 February 1992; in final form 25 March 1992

The rate constant of the NF_3 dissociation reaction in a helium mixture in the low-pressure limit was directly measured in a shock tube by a UV absorption method. The rate constant may be expressed as $K = 10^{14.38 \pm 0.07} \exp\{-[36600 \pm 2100\ (\text{cal/mol})]/RT\}$ $\text{cm}^3/\text{mol s}$ in the temperature range 1050–1600 K. Levels of the NF_3 stationary dissociation fraction were also measured as a function of the initial temperature of the mixture behind the shock wave. It increases monotonically with temperature and reaches 50% of the value at 1600 K, which corresponds to high NF_2 concentration up to 2×10^{17} cm^{-3}.

1. Introduction

Nitrogen trifluoride decomposition provides a significant source of fluorine atoms and NF_2 radicals for several branches of physico-chemical investigations, such as chemically pumped lasers for the IR spectral region [1], the generation of inert gas excimers [2], and the elaboration of chemical lasers for the visible spectral region [3]. The kinetics of NF_3 decomposition has not been accurately studied previously. In [4] the rate constant for NF_3 decomposition in a helium mixture has been measured in an electric discharge at 298 K. In refs. [5–8] decomposition of NF_3 in an argon mixture was studied in the shock tube, and the treatment of the experimental results was carried out by using an NF_3 decomposition mechanism description in terms of two reactions:

$$NF_3 + M \rightarrow NF_2 + F + M\,, \qquad (1)$$

$$NF_2 + F + M \rightarrow NF_3 + M\,. \qquad (2)$$

Other reactions which may occur in this system [5] were supposed to be negligible in the experimental conditions. Values of rate constants gained by different authors [5–8] are not in satisfactory agreement. These values at 1500 K vary from 3.5×10^6 $\text{cm}^3/\text{mol s}$ [6] to 4.5×10^9 $\text{cm}^3/\text{mol s}$ [7].

Correspondence to: N.N. Kudriavtsev, Moscow Institute of Physics and Technology, Dolgoprudny, Moscow Region 141700, Russia.

2. Experimental apparatus

In the present work thermal NF_3 decomposition in a helium mixture was studied behind reflected shock waves. The NF_2 radical concentration was monitored by UV absorption at 260 nm. Shock waves were generated in the stainless-steel shock tube (70 mm in diameter). Lengths of the driver and driven sections were 1 and 3.9 m, respectively. The gas temperature behind the reflected shock wave was calculated from the velocity of the incident shock wave measured on the 378 mm long base by means of two piezoelectric gauges. Pressure in the reacting mixture was measured by a piezoelectric pressure gauge located near the endplate. The spectrophotometric detection system consisted of a deuterium discharge lamp, quartz lenses to form the light beam, a 0.25 m grating monochromator and a photomultiplier. Signals from the photomultiplier and pressure gauge were displayed on the memorizing oscilloscopes.

3. Results

A mixture of NF_3 and helium in the ratio 1 : 10 was used in our experiments. Typical oscillograms of absorption and pressure behind the reflected shock

waves are represented in fig. 1 ((a) absorption, (b) pressure)). The time interval A–B on the oscillograms is considered to be a period of stationary conditions behind the reflected shock wave. The presence of a stationary plateau on the pressure oscillogram is connected with the isobaric progress of the chemical reactions.

The absorption oscillograms at the initial period of time have a linear region. Then the rate of increase of absorption becomes smaller, before reaching its stationary level. The duration of the existence of stationary conditions decreased from 780 to 450 μs and the duration of the linear region on the absorption oscillograms decreased from 80 to 10 μs with increasing temperature from 1050 to 1600 K. UV absorption in this system results from the NF_2 radical absorption band with its maximum near 260 nm [9,10]. The slope of the linear region on the absorption oscillogram is connected with the rate of reaction (1) at the initial time. Both the decrease in the NF_2 formation rate and stabilization of its concentration are caused by the influence of secondary reactions [5]. In such a manner, the values of the rate constants were measured in the temperature interval from 1050 to 1600 K and pressure interval from 0.7 to 2.3 atm. A plot of $\log K$ versus $10^4/T$ is in fig. 2. The values of rate constants at different pressures and the same temperature coincide within experimental error. From this it follows that reaction (1) proceeds as a second-order reaction in these conditions. The temperature dependence of the rate constant may be represented as

$$K = 10^{14.38\pm0.07} \times \exp\left(-\frac{36600\pm2100\ (\text{cal/mol})}{RT}\right) \text{cm}^3/\text{mol s}$$

for $T = 1050$–1600 K.

Comparison of the rate constant with the results of refs. [5–8] shows discrepancies both in the preexponential factor and activation energy. However, NF_3 was diluted by another inert gas (argon) in refs. [5–8]. Furthermore, the authors of refs. [5–8] used simplified kinetic models for NF_3 decomposition in treating their oscillograms. In the present work di-

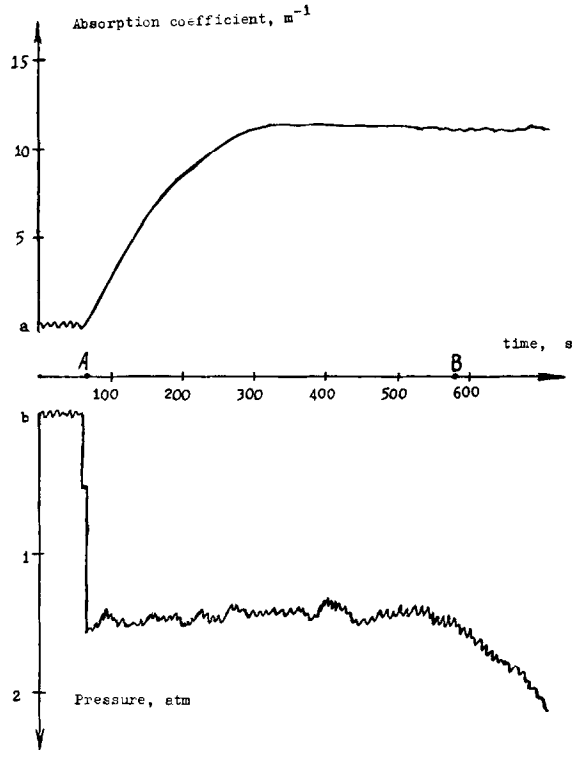

Fig. 1. Typical oscillograms of absorption and pressure behind the reflected shock wave; (a) absorption, (b) pressure.

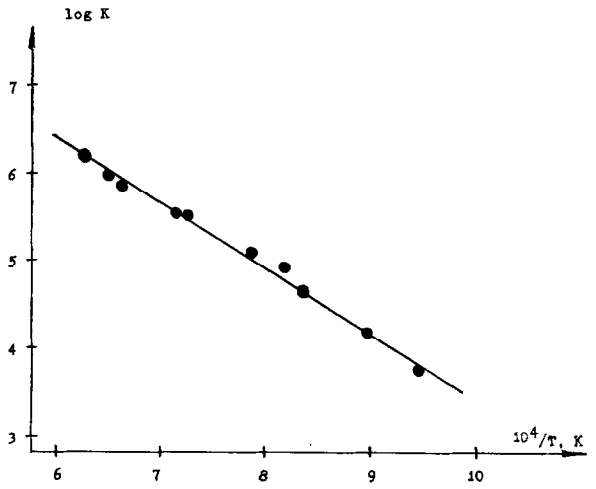

Fig. 2. Experimental values of $\log K$ versus $10^4/T$ (●) K is the rate constant of the dissociation reaction $NF_3+M \rightarrow NF_2+F+M$, T is the temperature behind the reflected shock wave. The best-fit straight line corresponds to an Arrhenius dependence $K = 10^{14.38\pm0.07}\exp\{-[36600\pm2100\ (\text{cal/mol})]/RT\}$ cm³/mol s in the temperature range 1050–1600 K.

rect measurements of the dissociation reaction (1) rate were actually performed.

The levels of stationary NF_2 UV absorption were also measured in our experiments. Experimental data are represented as a plot of the stationary dissociation fraction α versus the initial temperature behind the reflected shock wave in fig. 3. The dissociation fraction monotonically increases to the 50% level with temperature increasing to 1600 K. This level corresponds to the high concentration of NF_2 radicals 2×10^{17} cm^{-3}. It is necessary to mention that such an NF_2 concentration is supposed to be enough for the experimental realization of chemically pumped visible NF–IF laser models [3]. The use of NF_3 dissociation as a source of fluorine atoms and NF_2 radicals permits us to avoid the use of the unstable and expensive reagent tetrafluorohydrazine N_2F_4.

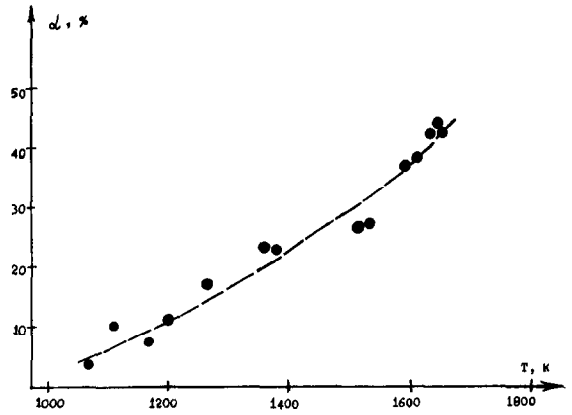

Fig. 3. Experimental values of the NF_3 stationary dissociation fraction versus $10^4/T$ (●). T is the temperature behind the reflected shock wave.

4. Conclusions

The rate constant of the NF_3 bimolecular dissociation reaction was measured by utilizing the shock tube technique in the temperature range from 1050 to 1600 K. Thermal NF_3 decomposition provides effective production of NF_2 radicals and fluorine atoms.

References

[1] A.S. Bashkin, V.I. Igoshin, A.N. Oraevsky and V.A. Shcheglov, Chemical lasers (Nauka, Moscow, 1982).
[2] R. Slater, Appl. Phys. B 42 (1987) 17.
[3] N.G. Basov, V.F. Gavrikov and V.A. Shcheglov, Kvantovaya Elektron. 14 (1987) 1754.
[4] M.A.A. Clyne and T.R. Watson, J. Chem. Soc. Faraday Trans. I 70 (1974) 1109.
[5] K.O. McFadden and E. Tschuikow-Roux, J. Phys. Chem. 77 (1973) 1475.
[6] E.A. Dorko, U.W. Grimm, K. Scheller and G.W. Mueller, J. Chem. Phys. 63 (1975) 3596.
[7] P.J. Evans and E. Tschuikow-Roux, J. Chem. Phys. 65 (1976) 4202.
[8] W.D. Breshears and P.F. Bird, J. Chem. Phys. 68 (1978) 2996.
[9] L.A. Kuznetsova, Yu.Ya. Kuzjakov and V.M. Tatevsky, Opt. i Spektroskopiya 16 (1964) 542.
[10] S.R. La Paglia and A.B.F. Duncan, J. Chem. Phys. 34 (1961) 1103.